Frequency reconfiguration of a dual-band phased array antenna with variable-impedance matching

Haider, N; Caratelli, D; Yarovoy, A

DOI
10.1109/TAP.2015.2441120

Publication date
2015

Document Version
Accepted author manuscript

Published in
IEEE Transactions on Antennas and Propagation

Frequency Reconfiguration of a Dual-Band Phased Array Antenna with Variable-Impedance Matching

Nadia Haider, Diego Caratelli, *Member, IEEE,* and Alexander G. Yarovoy, *Fellow, IEEE*

***Abstract*— In this article a dual-band phased-array antenna element is presented. The proposed element is particularly designed to possess frequency tuning capabilities by variable-impedance matching. It is demonstrated that the operational frequency band of the antenna shifts from L-band to S-band (about 2.5:1 frequency ratio) with in-band frequency tuning of about 25%. The compact size and the wide-angle scanning properties, make the antenna element suitable for phased-array application. Other advantages of variable-impedance matching for phased-array systems, such as sustain wider scan angles and minimize unwanted signal interferences, coming from spurious directions, are also discussed.**

***Index Terms*— variable impedance; frequency agility; reconfigurable antenna.**

I. INTRODUCTION

TRANSMISSION lines and connectors with 50 Ω characteristic impedance are extensively used to provide a standard interface between antennas, RF-frontends and measurement equipment. This standardization, however, severely limits the flexibility for RF-frontend and antenna design. The 50 Ω reference impedance value has several practical advantages, but is neither dictated by any severe physical limit nor does it assure the best performance for an electronic system. Historically, this impedance value was selected as a compromise between the minimum attenuation at around 77 Ω and the maximum power handling capability at around 30 Ω of an air-filled coaxial-line or waveguide [1]. However, having the liberty to choose another impedance value increases the design flexibility for both antennas and RF-frontends, and can enhance the total system performance dramatically [2-7]. Possibility to select reference impedances other than the 50 Ω value reveals the opportunity to use antenna structures for which the inherent input impedance is not 50 Ω [4]. In addition, [6-7] demonstrate improvements in gain and noise factor when the impedance of the RF-frontend is not obliged to match a single value.

Manuscript received March 25, 2014; revised January 15, 2015; accepted March 19, 2015.

N. Haider and A. G. Yarovoy are with Delft University of Technology, Microwave Sensing, Signals and Systems (MS3), 2628 CD Delft, The Netherlands (e-mail: nadia@nadiahaider.nl).

D. Caratelli is with The Antenna Company B.V., 2629 HD Delft, The Netherlands, and Tomsk Polytechnic University, 84/3 Sovetskaya Street, 634050 Tomsk, Russia.

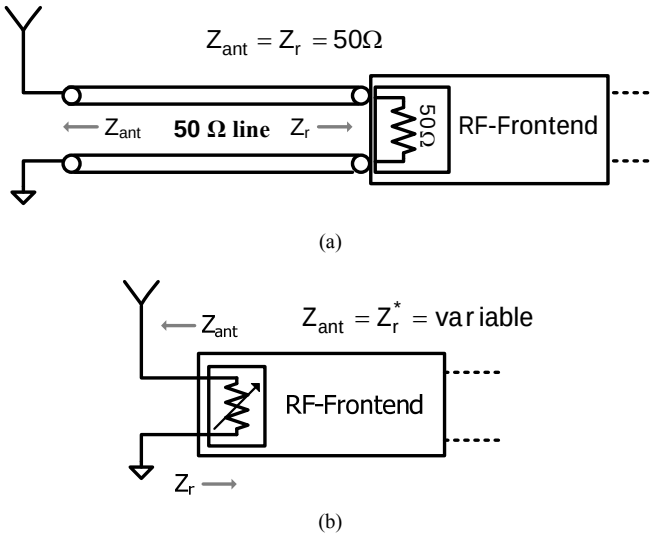

Fig. 1. (a) Conventional impedance-matching and (b) variable-impedance matching between antenna and RF-frontend. Here, * notation represents complex conjugate.

To further increase the performance, variable-impedance matching can be utilized. There are two possible approaches on variable impedance realization: one concept considers placing the variable components (e.g. pin-diodes and varactors) in the antenna element itself [8-10], while the alternative concept realizes antenna matching in transmit/receive (T/R) module. The main advantage of the former is in keeping interface between an antenna element and T/R module at 50 Ω and consequently an ability to use standard transmission lines in between, however the clear disadvantages are the increase of antenna complexity (and related to this increase of antenna system costs), parasitic influence of the control lines for tunable antenna elements and possible overall increase of the antenna element surface (leading to decreased scanning capabilities), additional ohmic losses in the control elements (up to 1–2 dB) and consequently reduction of maximal transmitted power. The latter approach requires impedance tunable RF-frontend with close integration with the antenna as illustrated in Fig.1b. This concept does not

lead to increase of antenna system complexity and its costs, does not limit maximal transmitted power and is actually free from other disadvantages of the first concept but its practical realization requires avoiding long transmission lines between antenna element and the T/R module, which is already a standard concept now in large phased-arrays up to X-band. Instead of a separate network [11-12], incorporating reconfigurable matching in the RF-frontend chip reduces the size and can provide a larger range of resistance and reactance values.

The remarkable advancements of the cellular industry have initiated immense interest in multi-standard radio. For these systems, designers are challenged to provide fully integrated reconfigurable RF-frontend [13]. Among other requirements, tunable input-impedance is a desired functionality. The study in [14] describes a 65 nm CMOS IC with on-chip low-resistance switches for input-impedance control. In [15] a low-loss adaptive matching network implemented in silicon-on-glass technology was demonstrated. Recently, impedance-tunable RF-frontends are also becoming commercially available [16-17].

These advancements in tunable RF technology give the opportunity to develop antenna systems with variable impedance matching that benefit from the high level integration between the antenna and the RF-frontend. An example of this technology is detailed in [18] where a broadband differential LNA (Low Noise Amplifier) designed for an active bunny-ear antenna array with non-standard input impedance is presented.

Although reconfigurable antennas have recently been studied for wide scope of applications [19-20], the concept of frequency reconfiguration by variable input-impedance of the RF-frontend did not gain wide research interest yet. Nevertheless, technological capabilities to tune the input impedance of RF modules are already available (e.g., the input impedance tunable 65 nm CMOS RF-frontend is presented in [14] and used to reconfigure the operational band of a microstrip antenna in [28]). In this article we investigate this concept by a dedicated antenna design for frequency reconfiguration between L and S radar-bands. A dual-band radiating element with two parallel E-slots has been developed to fully utilize the advantages of non 50 Ω variable-impedance matching. Having phased-array radar application in mind, the scanning properties of an electrically very large array with the proposed radiating elements have been thoroughly investigated. This article also emphasizes on a detailed description of the theoretical background of the variable-impedance approach and its advantages.

This manuscript is organized in six sections. We discuss the concept of variable-impedance matching and exemplify some of its major benefits in Section II. In Section III the theoretical analysis of power-wave theory is discussed. In Section IV the design of a frequency reconfiguration planar antenna by utilizing the variable impedance approach is presented. Section V discusses the advantages of the proposed design concept for phased-array antennas. Finally the conclusions are drawn in Section VI.

II. THE CONCEPT OF VARIABLE IMPEDANCE MATCHING

In Fig. 1 the concept of variable-impedance matching is illustrated. Unlike conventional fixed-impedance matching (Fig. 1a), here the input-impedance of the RF-frontend is tunable (Fig. 1b). Therefore, the input-impedances of both the antenna (Z_{ant}) and the RF-frontend (Z_r) are not obliged to be equal to a fixed value, typically 50 Ω, in order to minimize mismatch losses. Note that in Fig. 1b the 50 Ω transmission line is not included. Here, any transmission line (connecting the antenna to the RF-frontend) is now becoming a part of the antenna and is included in Z_{ant} in Fig. 1b. This requires that this line length has to be known in advance. However, a small variation in this length (less than one twentieth of the wavelength) has in practice negligible influence on the antenna input-impedance.

This concept of variable-impedance matching has many fundamental advantages. For instance, many antenna elements show high radiation efficiency outside their instantaneous frequency band. As input impedances of most antennas are highly frequency dependent, a fixed 50 Ω impedance transformation only allows a good matching within a limited frequency range. For the concept presented in Fig. 1b, the input-impedance of the RF-frontend (Z_r) can be changed to match the antenna input-impedance (Z_{ant}). In this way, frequency reconfigurable or tunable antennas can be easily realized. This approach is useful to support different communication standards, compensate for antenna mismatch losses due to aging or detrimental effects of objects in the close vicinity of the antenna (particularly important for hand-held cellular devices) or reduce any mismatch caused by manufacturing processes.

The approach can also be applied in selecting sub-bands of wideband or multi-band antenna systems. This can be achieved by matching the frontend to the corresponding impedance of a specific band while suppressing the signals from other bands through intentional mismatch. This will provide band selectivity, decrease out-of-band signals, reduce the noise bandwidth and relax the constraints on the frontend filters. Furthermore, the proposed concept is helpful for phased-array antennas to maintain good matching over large scan angles and thereby increase scan volume. On the contrary, angle dependent input-impedance matching provides the opportunity to perform spatial-filtering and thereby reduces interfering signal levels impending from adjacent angles.

Owing to these benefits there is a strong possibility that in future, variable-impedance matching will extensively be used for many applications, for example communications, cognitive radio, radio astronomy and radar.

III. THE THEORY OF POWER WAVES FOR VARIABLE IMPEDANCE MATCHING

In this section, the theoretical formulation backing the variable impedance matching approach is described and discussed in detail.

In the theory of microwave circuit, the concept of travelling waves is a useful and straightforward method to provide a physical explanation for many phenomena occurring in transmission lines. Travelling waves were introduced by applying linear transformations to voltages and currents and they provide a meaningful physical understanding of waves travelling in two opposite directions along a transmission line. The travelling waves are defined as,

$$a_t = \frac{\sqrt{ReZ_r}}{2|Z_r|}(V_i + Z_r I_i),\ b_t = \frac{\sqrt{ReZ_r}}{2|Z_r|}(V_i - Z_r I_i) \quad (1)$$

where, a_t and b_t are the travelling waves moving towards and from the i^{th} port respectively, while V_i and I_i are the voltage and current amplitudes flowing into the corresponding port. In (1) Z_r denotes the reference impedance, or, in other words, the impedance seen from the i^{th} port looking towards the transmission line. The time-average real power delivered to the antenna can be computed as,

$$P_{ant} = \frac{1}{2}Re(V_i I_i^*)$$
$$P_{ant} = \frac{1}{2}(|a_t|^2 - |b_t|^2) - \frac{ImZ_r Im(a_t^* b_t)}{ReZ_r} \quad (2)$$

From (2) we know that for a complex value of $Z_r$the total delivered power cannot be expressed straightforwardly as the difference in power carried by the incident and reflected travelling waves [21].

In order to allow for a more insightful analysis of the general case involving complex reference impedances, different formulations based on suitable linear transformations of port voltages and currents were proposed [21-25]. Among them, special attention is to be given to the concept of power wave which provides a more consistent description of the propagation of power in transmission lines and was introduced in [22-23] as,

$$a_p = \frac{V_i + Z_r I_i}{2\sqrt{ReZ_r}},\ b_p = \frac{V_i - Z_r^* I_i}{2\sqrt{ReZ_r}} \quad (3)$$

where, a_p and b_p are the power waves moving towards and from the i^{th} port respectively. In this case, the total power delivered to the antenna can be expressed as the difference in power carried by the incident and reflected power waves,

$$P_{ant} = \frac{1}{2}\left(|a_p|^2 - |b_p|^2\right) \quad (4)$$

When the reference impedance (in this case Z_r) is complex, the power-wave definition of reflection coefficient is more meaningful than the more commonly used travelling-wave definition. The reflection coefficient for power waves has been derived in [22] as,

$$\Gamma_p = \frac{b_p}{a_p} = \frac{Z_{ant} - Z_r^*}{Z_{ant} + Z_r} \quad (5)$$

Equation (5) shows that Γ_p is zero when the antenna and the RF-frontend impedances are complex conjugates of each other. It this case, there is no reflected power wave (b_p) and maximum power will be delivered to the antenna for radiation. It is worth pointing out here that the conventional travelling-wave-based definition of reflection coefficient,

$$\Gamma_t = \frac{b_t}{a_t} = \frac{Z_{ant} - Z_r}{Z_{ant} + Z_r} \quad (6)$$

does not satisfy the above mentioned condition and fails to provide a physical meaning when the reference impedance is complex. In addition, as explained in [23] for (6) the magnitude of reflection coefficient can be larger than unity even for a passive system. On the other hand, the magnitude of the power-wave reflection coefficient is smaller than unity, that is $|\Gamma_p| < 1$, provided that the real parts of Z_{ant} and Z_r have the same signs, as always expected for passive devices.

Despite the fact that the theory of power wave has been introduced many decades ago, it is still not widely used by the antenna and microwave engineer community (some applications of power wave method are seen for RFID tag design [26]). For commonly used fixed 50 Ω impedance-matching one can resort to the much simpler travelling wave theory. However, for a co-design of antenna with the RF-frontend where the impedance is not limited to any real values, a correct understanding of the power-wave theory is crucial.

IV. FREQUENCY RECONFIGURATION WITH VARIABLE IMPEDANCE MATCHING

In this section, the concept of variable-impedance matching is applied to tune the antenna's operational frequency over a large band. For dual- or multi-band antennas, an operational band can be selected by matching the frontend to the corresponding antenna input impedances within a specific band while suppressing, in this way, the signals from other bands by deliberate mismatch. For this investigation, an E-slot microstrip antenna is presented for which the operating frequency can be shifted from L-band to S-band by using the variable impedance matching approach discussed in the previous sections.

A. The E-Slot Antenna Topology

The physical layout of the E-slot antenna is sketched in Fig. 2. The proposed antenna mainly differs from conventional microstrip antennas by having the double E-slots and a blind-via feeding.

Dual-band planar antennas are commonly realized by inserting slots in the radiating structure [27]. This approach provides the opportunity to control the operating band of the TM_{030} mode and to transform the three-lobe radiation pattern of this mode to the desired single-lobe pattern.

In comparison with two parallel slots [27], the proposed E-slot structure separates the TM_{010} mode and the TM_{030} mode over a wider frequency band. The parameter w_e (see Fig. 2b)

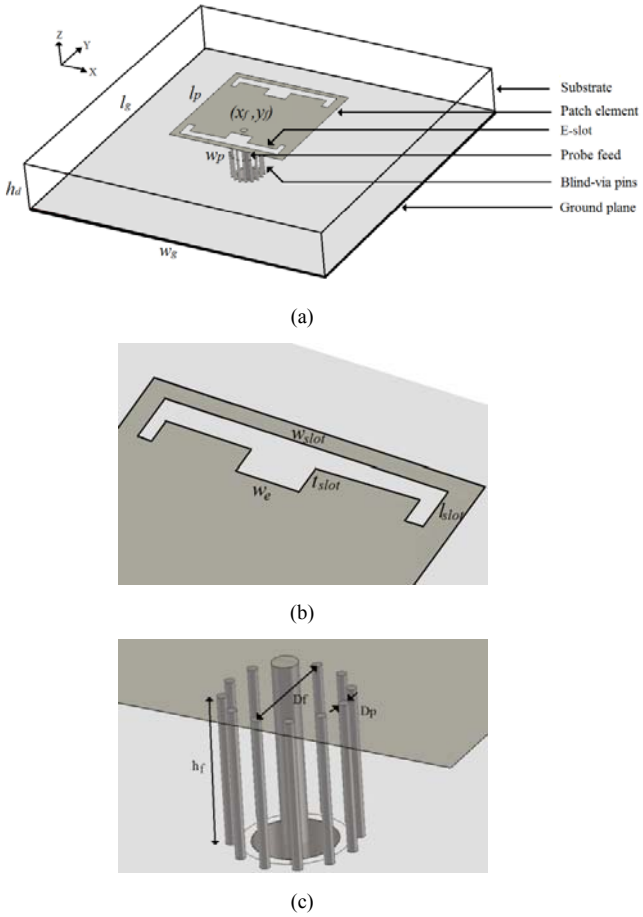

Fig. 2. E-slot antenna (a), the slot section (b) and the feeding section (c). Geometrical characteristics of the structure: w_p=34 *mm*, l_p=35 *mm*, w_g=90 *mm*, l_g=90 *mm*, h_d=9 *mm*, x_f=0 *mm*, y_f=-5.5 *mm*, w_e=5 *mm*, w_{slot}=33 *mm*, l_{slot}=6.5 *mm*, t_{slot}=4.5 *mm*, D_f=5 *mm*, h_f=7.6 *mm*, D_p=0.5 *mm*. The number of vias in the fence is 11, and the diameter of the center probe is 1.28 *mm*. The origin of the adopted coordinate system is located at the center of the radiating patch.

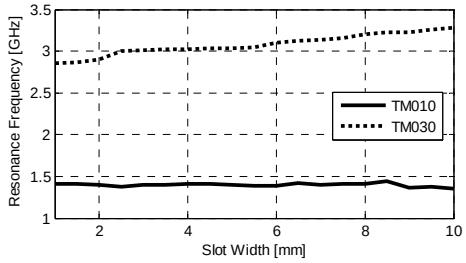

Fig. 3. Simulated results of the resonance modes vs central slot width (W_e)

influences the current path of the third harmonic (TM_{030} mode) due to high surface current distribution at these locations. Increasing this value leads to a shorter current path for the TM_{030} mode and thereby swifts the resonating frequency towards the upper band. On the other hand, the central slots only marginally affect the first harmonic (TM_{010}mode) as the current density of the subsequent mode is particularly low at the slot locations. In Fig. 3 the effect of the slot width (w_e) on the frequency ratios of the two aforesaid modes is depicted. By controlling the width of the central slot we can influence the frequency band of the TM_{030} mode. It is evident in Fig. 3 that TM_{010} mode remains unaffected by the variations of this parameter.

B. Blind-via Feeding Section

The blind-via feeding section is shown in Fig. 2c. A detailed study of the proposed feeding structure for a single-band microstrip antenna is presented in [29]. The effect of the proposed feeding structure on the reference antenna element is discussed here for completeness.

It is known that the input impedance of an antenna element fed by a probe possesses a large reactive part. For the proposed E-slot microstrip antenna this reactive value is particularly high for the TM_{030} mode for which the thickness of the dielectric substrate relative to the wavelength is large compared to the TM_{010} mode.

A high reactive input impedance of the antenna makes it difficult to match the device to the RF-frontend. By minimizing the effective length of the probe-feed the reactive part of the input impedance can be reduced. To achieve this goal, a via-pin fence can be used to encircle the probe resulting in a coaxial-line-like section partly slipped in the antenna substrate (see Fig. 2c). The obtained results illustrate that the BV fence structure significantly reduces the antenna input reactance and flattens the antenna resistance around the TM_{030} mode. Furthermore, geometrical parameters (in particular the fence diameter D_f) of the fence can be used to control the input impedance of the antenna.

C. Antenna Performance

Based on the antenna architecture discussed in the previous section, an antenna element with high radiation efficiency in L- and S-radar bands (1.2-1.4 GHz and 2.9-3.5 GHz) was designed. The antenna is etched on Rogers high-frequency material, RO4003, with ε_r= 3.5. The prototype of the antenna is presented in Fig. 4. For the experimental data the Agilent E8364B network analyzer was used. The length and the width of the radiating element here are less than $\lambda_0/6$, λ_0 being the free-space wavelength of the first harmonic (1.4 GHz).The size of the antenna element was reduced by avoiding air-

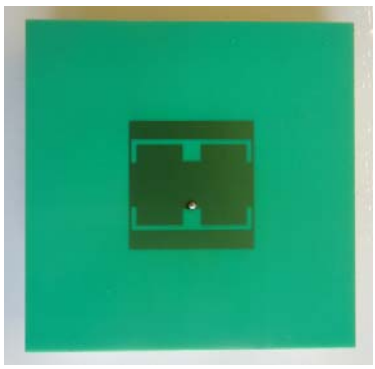

Fig. 4. E-slot microstrip antenna prototype

substrate and by increasing the thickness of the dielectric substrate up to 9 mm. The antenna compact size makes it suitable for dense array environment.

The measured input impedance of the antenna is compared with the simulation results and a close agreement was observed (Fig. 5). The fundamental mode (TM_{010} mode) resonates at 1.45 GHz. Around the fundamental mode we notice two circuitry resonances (peaks in the real part of the input impedance curve and zeros in the imaginary part) caused by loading the patch with complex-valued impedance of the slots. These resonances however do not correspond to excitation of new current modes on the patch. The second (TM_{020}) and the third (TM_{030}) harmonics are efficiently excited around frequencies of 2 GHz and 3 GHz, respectively. Due to the presence of the E-slots, the higher order harmonics are shifted towards the lower frequency range.

The measured and simulated boresight absolute gains (which do not consider any reflection occurring at the feeding location) of the antenna are plotted in Fig. 6. Around 1.45 GHz and 3 GHz the antenna's absolute gain reaches the local maxima as a result of radiation of the fundamental and the third harmonic modes, respectively. The measured absolute gain is 6.8 dBi at 1.47 GHz while it is 5.4 dBi at 3 GHz. It should be pointed out here that the absolute gain remains higher than 3 dBi from 1.05 GHz to 1.55 GHz and again from 2.7 GHz to 3.2 GHz. Due to relatively thick substrate, the antenna radiation efficiency decreases with frequency from approximately 95% at 1.5 GHz to 82% at 3.5 GHz. This indicates adequate radiation efficiencies at the aforementioned frequency bands. Here, the antenna gain values are slightly less than that for a conventional patch (about 6.0-6.5 dBi) due to the reduced antenna aperture at the lower band and the surface-wave loss at the upper band.

The measured and the simulated reflection coefficients of the antenna for two different input-impedance settings as typical examples are shown in Fig. 7. In this example, the frequencies for which the absolute gain reaches its maximal values are selected. Here, the experimental data is measured for 50 Ω reference impedance and the input-reflection coefficient for other impedance values were extracted according to (4). Fig. 7 reveals that by changing the reference input impedance from about 10 Ω to 75 Ω (both in simulations and post-processing of the experimental results) the operating frequency can be shifted from L to S band. The realization and the details of an input-impedance tunable RF-frontend are discussed in [11] and [28] where a 65 nm CMOS RF-frontend was used to tune the operational band of a microstrip antenna.

Fig. 5 shows that within the radar L-band (1.2 GHz – 1.4 GHz) the input-impedance varies rapidly with frequency. This provides opportunity to tune the operational band by proper impedance matching. For the E-slot antenna, the input-impedance of the antenna is inductive within the above mentioned band. It is worth mentioning here that inductive antenna impedances are often advantageous for conjugate matching since in an integrated circuit capacitive

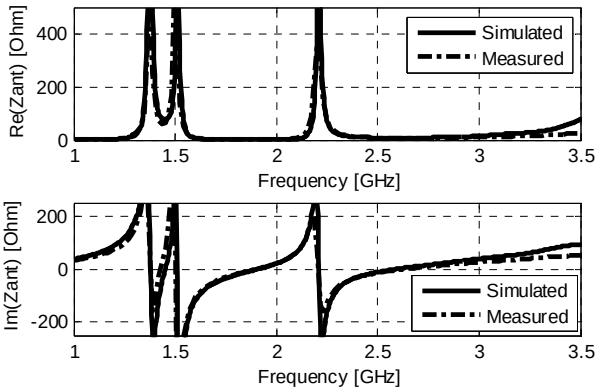

Fig. 5. Input-impedance of the E-slot microstrip antenna

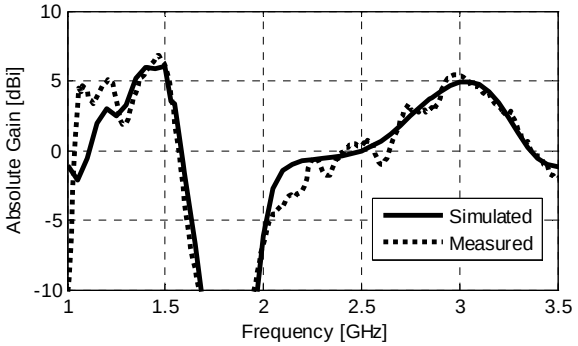

Fig. 6. Boresight absolute gain as a function of frequency

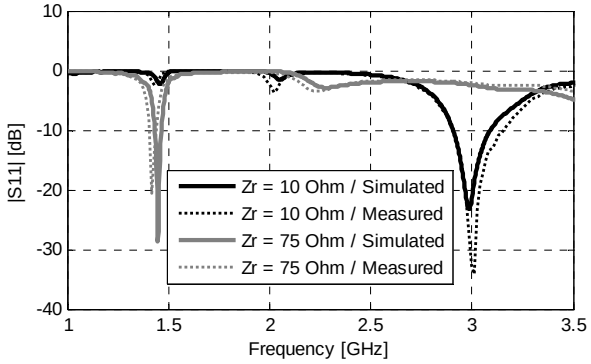

Fig. 7. Simulated and measured power wave reflection coefficient for two different impedance settings

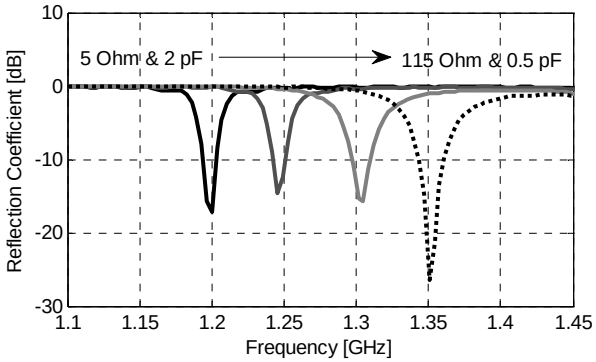

Fig. 8. Power-wave reflection coefficient for various complex reference impedance settings

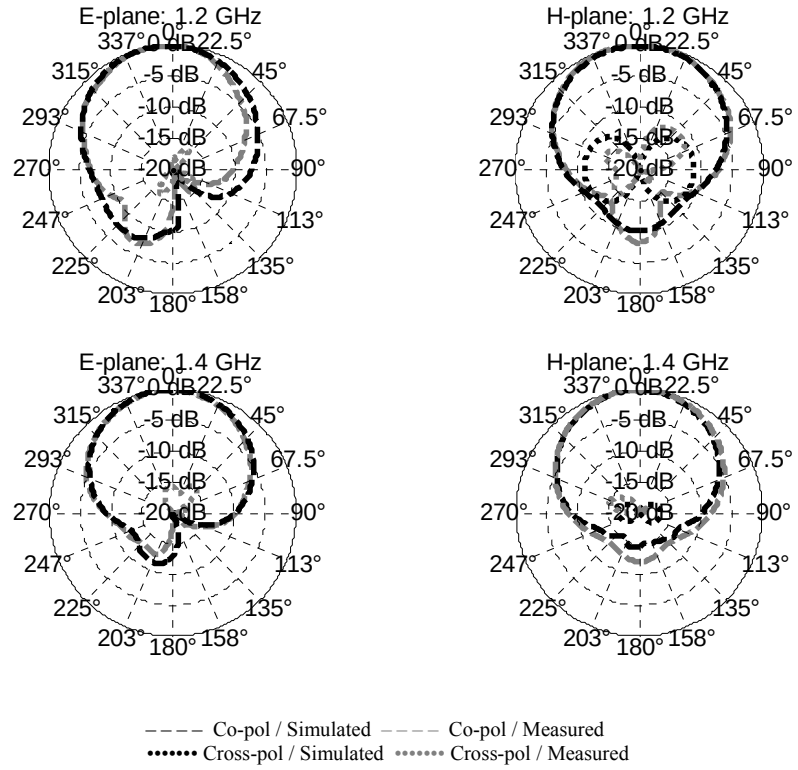

Fig. 9. Normalized radiation patterns at L-band

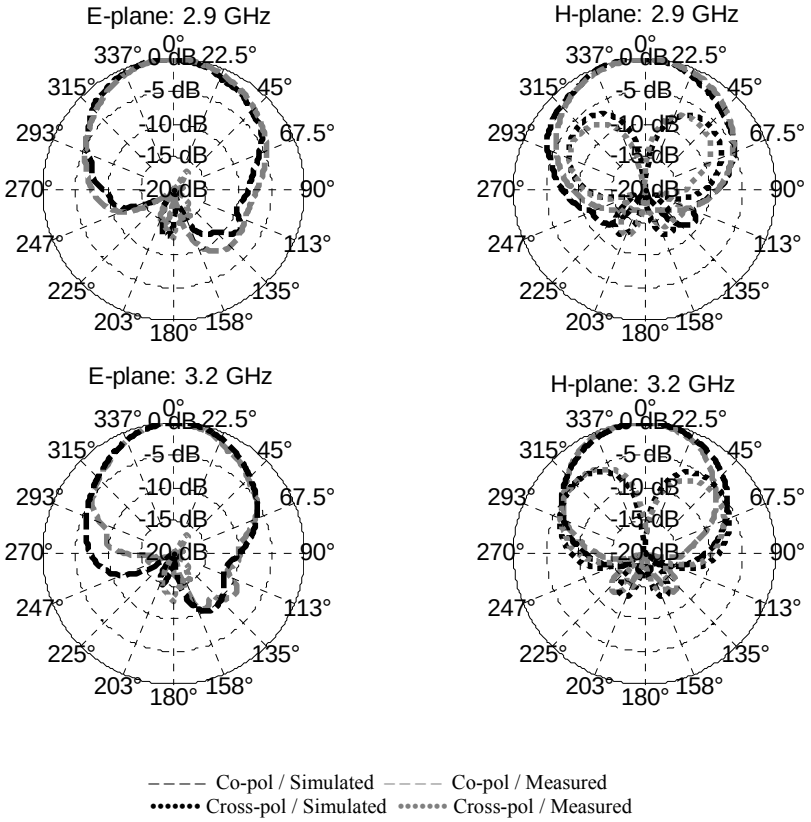

Fig. 10. Normalized radiation patterns at S-band

impedances are easier to synthesize compared to inductive ones. In Fig. 8 it is shown that the operational band shifts towards the higher frequencies when the resistive part of the input impedance increases while the reactive part decreases.

The far-field radiation patterns are presented in Figs. 9-10. Measured and theoretical results indicate low cross-polarization levels for the lower band. At the higher band the cross-polarization levels increase for H-plane due to the larger electrical thickness of the dielectric substrate. Furthermore, symmetric radiation patterns for both upper and lower frequency bands are evident owing to the symmetrical geometry of the antenna.

V. VARIABLE-IMPEDANCE MATCHING FOR PHASED-ARRAY ANTENNAS

It is widely known that the active impedance of a phased-array antenna varies with the scan angle and the scale of this variation depends on the amount of the couplings between the radiating elements. As a result, a single predefined reference impedance value gives an optimal impedance matching for a single beam direction (usually for boresight scanning). For other directions the reflected signal increases due to impedance mismatch.

Generally, the variation of the active impedance is minimized by reducing the antenna mutual couplings with proper antenna design and optimization. However, the outcome of such approach is highly design specific. To alleviate this problem utterly, a scan dependent variable-impedance matching is desired [30]. This can be realized by changing the input-impedance of the RF-frontend not only as a function of the desired band, but also if needed, as a function of the scan angle.

To investigate the concept of scan dependent matching, an infinite array of E-slot elements with triangular grid was analyzed. The numerical model of the infinite array is illustrated in Fig. 11 where an element spacing of 53.6 mm was selected to allow ±60° grating-lobe free scan angle up to 3 GHz. The current work is done having in mind electrically

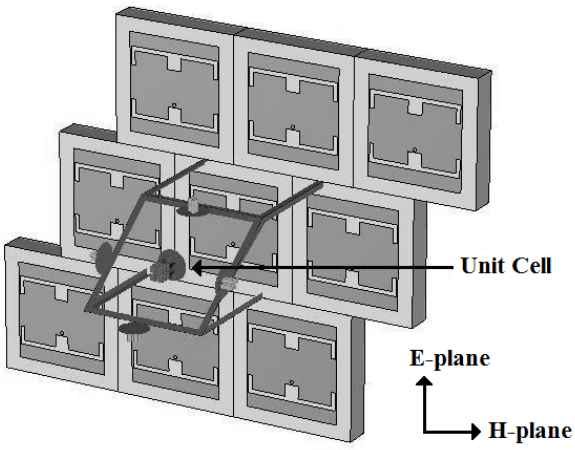

Fig. 11 E-slot infinite array configuration with 53.6 mm element periodicity

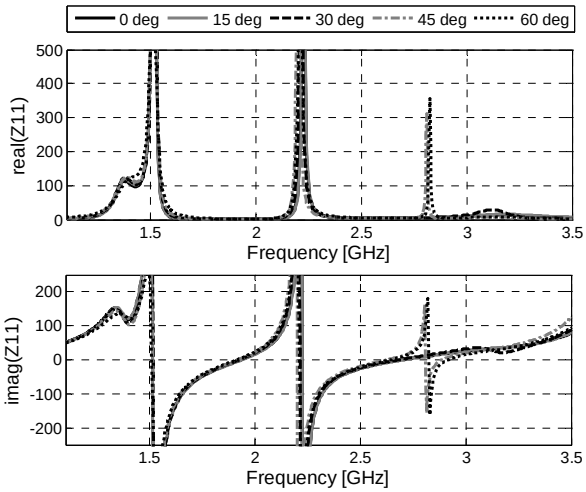

Fig. 12 E-plane active input impedance versus frequency for various scan angles

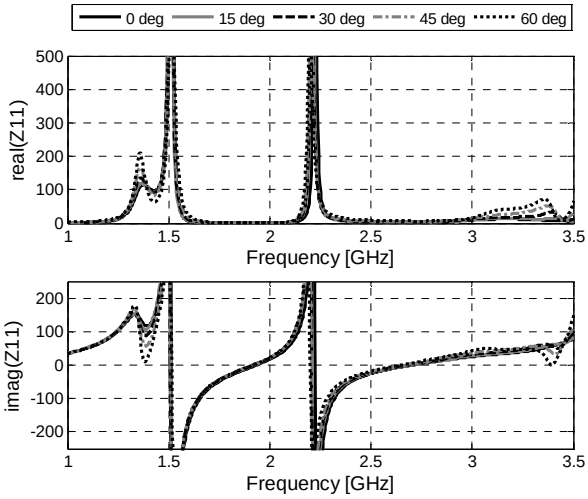

Fig. 13 H-plane active input impedance versus frequency for various scan angles

very large arrays with thousands of radiating elements. The infinite array analysis is useful to evaluate the active-element impedances of such large arrays. However, it is worth noting here that the performances of elements close the edge of a finite array will be different from the element within an infinite array.

In Fig. 12 and Fig. 13 the active input impedances of the antenna are shown for different scan angles. Along the E-plane coupling with the adjacent elements are less due to the triangular array arrangement. Hence, the impedances remain more stable with the frequency within the operational bands. In Fig. 13 we notice that along the H-plane the impedance variation is higher for the L-band in comparison with the S-band (at lower frequency the electrical distance between the elements is smaller resulting in a larger coupling). The scan-angle (θ) dependency of the impedances can be expressed with polynomial functions as follows:

$$Z^{real}(f,\theta) = C_0^{real}(f) + C_1^{real}(f).\theta + C_2^{real}(f).\theta^2 + ... + C_N^{real}(f).\theta^N \quad (7)$$

$$Z^{imag}(f,\theta) = C_0^{imag}(f) + C_1^{imag}(f).\theta + C_2^{imag}(f).\theta^2 + ... + C_N^{imag}(f).\theta^N \quad (8)$$

where C_{0-N} are the polynomial coefficients. As the variation in the impedances is not abrupt, a third order (N=3) polynomial function can estimate these values with about 0.97 correlation of determination. Note that the ability to analytically express the scanning behavior of the antenna with polynomial functions will significantly reduce the total number of numerical analysis necessary for the co-design of the antenna and RF-frontend. To extract the equivalent mathematical expression, numerical active-impedances of only five scanning angles (0°, 15°, 30°, 45°, 60°) were used. Fig. 14 shows the H-plane active input impedances as a function of the scanning angle at 1.37 GHz as a typical example. Here we observe a nearly perfect fit to the data curve.

In Fig. 15 the frequency-domain behavior of the coefficients C_{0-N}, conveniently expressed as 6th-order polynomial functions, is shown. For f < 1.3 *GHz*, the higher order coefficients become negligible (resulting in an almost constant value of impedances). On the contrary, for f > 1.3 *GHz* these coefficients become larger. In this context, it is worth noting that the C_0 coefficient reveals the frequency-domain behavior of the antenna input-impedance for 0° scanning angle.

In Fig. 16 the active reflection coefficients are illustrated. Here these active reflection coefficients are computed according to (4). In Fig. 16(a) the reference impedances were considered constant for all scan angles and were selected to provide an optimal matching condition at θ=0° angle at 1.37 GHz. Here, we notice that the reflection coefficient increases with the scan-angle. Note that within the operational bands, the highest variation in active impedance is around 1.37 GHz.

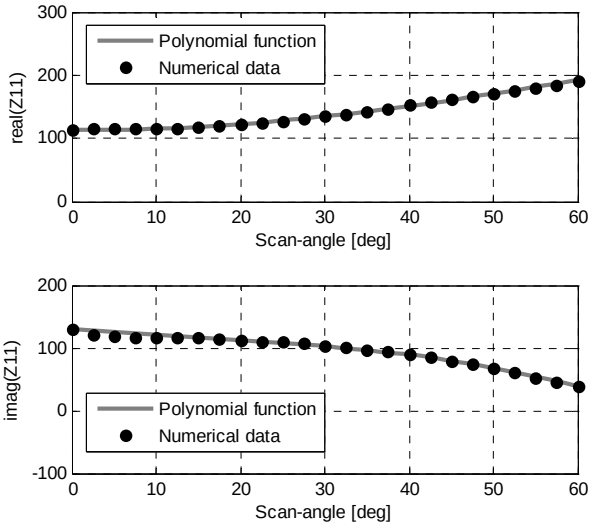

Fig. 14 H-plane active input impedance versus scan-angle at 1.37 GHz

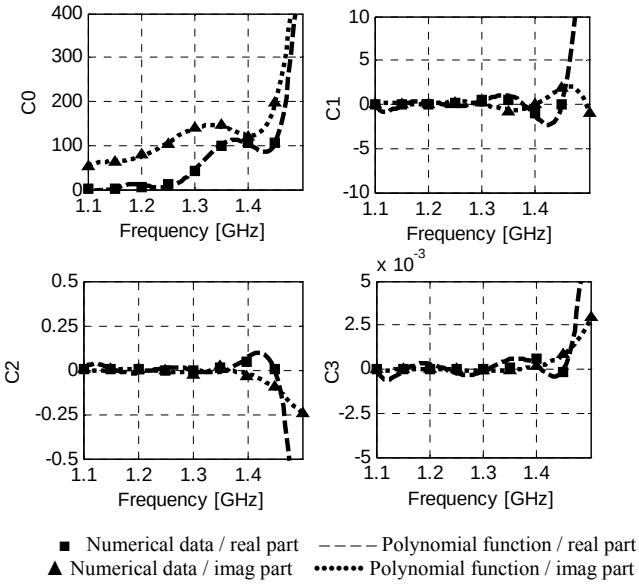

Fig. 15 Polynomial coefficients of equations (7) and (8) for H-plane as a function of the frequency

If further improvement of the matching condition is desired for the utmost scan angles, an impedance matching where the reference impedance will vary with the scan angle is required. Fig. 16(b) provides an illustration of this approach. Here, the reference impedance is conjugate-matched to the corresponding active-antenna impedances and hence reduction of the active reflection coefficients are observed for off-boresight angles (the active-antenna impedances at 1.37 GHz are presented in Fig. 14). In this example, the reference impedance is set to provide a minimum reflection at 1.37 GHz. As a result the realized gain is maximized. In this case, the realized gain of each element can be improved by 0.6 dB for θ=60°. Fig. 16(b) reveals that the active-impedance bandwidth (at -10 dB level) is 50 MHz. This bandwidth can be improved at the expense of reduced matching, known from the Bode-Fano criterion [31-32].

This approach of scan dependent impedance matching is helpful for phased-array antennas to maintain good matching over large scan angles. In addition to this advantage of sustaining better matching, the proposed approach has another potential for phased-array systems. An angle dependent input-impedance matching provides the opportunity to perform some spatial-filtering. Any signal approaching from directions other than the main beam will undergo larger suppression. This will assist beam forming networks to minimize the interferences of unwanted signals impending from adjacent angles.

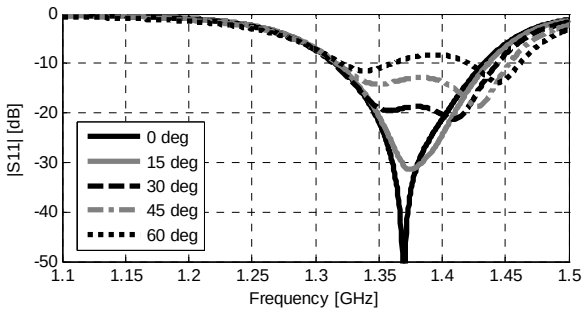

(a)

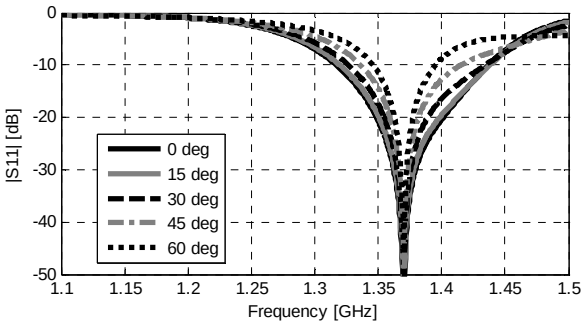

(b)

Fig. 16 Magnitude of active reflection coefficient versus frequency along H-plane for (a) reference impedance conjugate-match to the active input impedance of the antenna for θ=0° at 1.37 GHz (Z_r = 114 – 130j) and (b) reference impedance conjugate-match to the corresponding active antenna impedances at 1.37 GHz (shown in Fig. 14)

VI. CONCLUSION

This paper discusses and verifies advantages of having a variable-impedance matching between the antenna and the RF-frontend. The concept of antenna frequency reconfiguration by variable impedance matching was, in particular, implemented to an E-slot planar antenna. This antenna possesses dual- (L- and S-) band operation based on radiation of the fundamental (TM_{010}) mode and the third harmonic (TM_{030}). We showed that the antenna's operational band can be switched from L- to S-band (about 2.5:1 frequency ratio) by changing the reference impedance. In addition, operational frequency shift of about 25% within L-band is possible by proper tuning of the reference impedance. The E-slot antenna considered is an attractive solution for frequency reconfigurable (phased-) array due to its ability to switch from L- to S- (radar) bands, compact size of 35 x 34 mm^2, symmetric radiation patterns, back feeding technique and wide-angle scanning capabilities.

Furthermore, we demonstrate that the variable-impedance matching might provide substantial advantages to phased-array systems. In particular, a scan-angle dependent impedance control of the RF-frontend will diminish the fundamental active-impedance matching problem and thereby increase the scan volume. At the same time a scan dependent matching will further enhance system performance and robustness by reducing interfering and jamming signals impinging from adjacent angles. Finally, it is well-known that elements close to the edge of an array have active impedance essentially different from those located in the center. Dummy elements along the array borders are often used when a conventional 50 Ω impedance matching is applied. These dummy elements reduce the overall gain. An impedance-tunable RF-frontend can provide a particular impedance matching for these edge elements and thereby avoid the use of non-active dummy elements.

ACKNOWLEDGMENT

This research is conducted as part of the Sensor Technology Applied in Reconfigurable systems for sustainable Security (STARS) project. For further information: www.starsproject.nl.

The authors gratefully acknowledge the support of Mark Oude Alink and Eric Klumperink. The authors also wish to thank Antoine Roederer and Bert Jan Kooij for many useful discussions, and Johan Zijderveld and Pascal Aubry for their support during the antenna measurements. PCLL (Printech Circuit Laboratories Ltd) is acknowledged for its help in the antenna prototype fabrication.

The authors also thank to anonymous reviewers, whose suggestions and questions helped to improve the paper.

REFERENCES

[1] D. M. Pozar, *Microwave Engineering*, 3rd ed., John Wiley & Sons, Inc, NJ, 2005, pp.130

[2] K.F. Warnick and M.A. Jensen, "Signal and noise analysis of small antennas terminated with high-impedance amplifiers," *2nd European Conf. on Antennas Propag.*, Edinburgh, Nov. 2007.

[3] V. Kaajakari, A. Alastalo, K. Jaakkola and H. Seppa, "Variable antenna load for transmitter efficiency improvement," *IEEE Trans. Microw. Theory Tech.*, vol.55, no.8, pp.1666-1672, Aug. 2007.

[4] Formato, R.A.: 'Variable Z0 antenna device design system and method'. U.S. patent 0331436, Dec. 2012.

[5] S. Bagga, A.V. Vorobyov, S.A.P Haddad, A.G. Yarovoy, W.A. Serdijn, J.R. Long, "Co-design of an impulse generator and miniaturized antennas for IR-UWB", *IEEE Trans. Microw. Theory Tech.*, vol. 54, no. 4, pp. 1656-1666, Apr. 2006.

[6] E.A.M. Klumperink, Qiaohui Zhang, G.J.M. Wienk, R. Witvers, J.G. bij de Vaate, B. Woestenburg and B. Nauta, "Achieving wideband sub-1dB noise figure and high gain with MOSFETs if input power matching is not required," *IEEE Radio Frequency Integrated Circuits (RFIC) Symp.*, pp.673-676, Jun. 2007.

[7] M. Pelissier, et al, "LNA-antenna codesign for UWB systems", *Circuits and Systems, 2006. ISCAS 2006. Proceedings. 2006 IEEE International Symposium on*, May 2006.

[8] Y. Tawk, J. Costantine, and C. G. Christodoulou, "A varactor-based reconfigurable filtenna," *IEEE Antennas and Wireless Propagation Letters*, vol. 11, pp. 716–719, Jul. 2012.

[9] S. V. Hum and H. Y. Xiong, "Analysis and design of a differentially-fed frequency agile microstrip patch antenna," *IEEE Trans. on Antennas Propag.*, vol. 58, no. 10, pp. 3122–3130, Oct. 2010.

[10] R.B. Waterhouse, and N.V. Shuley, "Scan performance of infinite arrays of microstrip patch elements loaded with varactor diodes," *IEEE Trans. on Antennas Propag.*, vol. 41, no. 9, pp. 1273–1280, Sep. 1993.

[11] M.J. Franco and D. Dening, "Broadband reconfigurable matching network of reduced dimensions for the UHF military satellite

communication band," in *IEEE MTT-S International Microwave Symp. Dig.*, Jun. 2011.

[12] Yue Li, Z. Zhang, W. Chen, Z. Feng and M.F. Iskander, "A switchable matching circuit for compact wideband antenna designs," *IEEE Trans. on Antennas Propag.*, vol.58, no.11, pp. 3450-3457, Nov. 2010.

[13] F. Agnelli et al., "Wireless multi-standard terminals: System analysis and design of a reconfigurable RF front-end," *IEEE Circuits Syst. Mag.*, pp. 38–59, 1st Quarter, 2006.

[14] M. S. Oude Alink, E. A. M. Klumperink, A. B. J. Kokkeler, Z. Ru, W. Cheng and B. Nauta, "Using crosscorrelation to mitigate analog/RF impairments for integrated spectrum analyzers," *IEEE Trans. Microw. Theory Tech.*, vol.61, no.3, pp.1327-1337, Mar. 2013.

[15] K. Buisman, L. C. N. de Vreede, L. E. Larson, M. Spirito, A. Akhnoukh, Y. Lin, X. Liu, and L. K. Nanver, "Low-distortion, low-loss varactor-based adaptive matching networks, implemented in a silicon-on-glass technology," in *Proc. RFIC Symp.*, Long Beach, CA, pp. 389–392, Jun. 2005.

[16] http://www2.imec.be/content/user/File/NEW/Research/Wireless%20Communication/Analog%20R_F%20front-end/Scaldio%20leaflet.pdf

[17] http://www.st.com/web/en/resource/technical/document/datasheet/DM00033029.pdf

[18] O. García-Pérez, D. Segovia-Vargas, L. E. García-Muñoz, J. L. Jiméenez-Martín, and V. González-Posadas, "Broadband differential low-noise amplifier for active differential arrays," *IEEE Trans. Microw. Theory Techn.*, vol. 59, no. 1, pp. 108–115, Jan. 2011.

[19] J. T. Bernhard, "Reconfigurable antennas," in Synthesis Lectures on Antennas, Morgan and Claypool Publishers, 2007.

[20] R. L. Haupt and M. Lanagan, "Reconfigurable antennas," *IEEE Antennas Propag. Mag.*, vol. 55, no. 1, pp. 49–61, Feb. 2013.

[21] R. B. Marks and D. F. Williams, "A general waveguide circuit theory," J. Res. Nat. Inst. Standards Technol., vol. 98, no. 5, pp. 533-561, Sep. 1992.

[22] K. Kurokawa, "Power waves and the scattering matrix," *IEEE Trans. Microw. Theory Tech.*, vol. MTT-13, no. 3, pp. 194–202, Mar. 1965.

[23] K. Kurokawa, *An Introduction to the Theory of Microwave Circuits*, Academic press, Inc, NY, 1969, pp.33-38.

[24] D. C. Youla, "On scattering matrices normalized to complex port numbers," Proc. IRE, vol. 49, no. 7, pp. 1221–1221, Jul. 1961.

[25] J. Rahola. "Power waves and conjugated matching," *IEEE Trans. Circuits Syst. II*, vol. 55, no. 1, pp.92-96, Jan. 2008.

[26] P.V. Nikitin, K.V.S. Rao, S.F. Lam, V. Pillai, R. Martinez and H. Heinrich, "Power reflection coefficient analysis for complex impedances in RFID tag design," *IEEE Trans. Microw. Theory Tech.*, vol.53, no.9, pp. 2721-2725, Sep. 2005.

[27] S. Maci, G. Biffi Gentili, P. Piazzesi and C. Salvador, "Dual-band slot-loaded patch antenna," *Microwaves, Antennas and Propagation, IEE Proceedings*, vol.142, no.3, pp. 225-232, Jun. 1995.

[28] N. Haider, M. S. Oude Alink, D. Caratelli, E. A. M. Klumperink and A. G. Yarovoy, "Frequency-tunable antenna by input-impedance-tunable CMOS RF-frontend," *European Microwave Integrated Circuits Conference (EuMIC),* Nuremberg, Oct. 2013.

[29] N. Haider, D. Caratelli, and A. G. Yarovoy, "Blind-via fence for bandwidth enhancement of planar pin-fed antennas," *IET Microwaves, Antennas and Propagation*, submitted.

[30] P. W. Hannan, D. S. Lerner, and G. H. Knittel, "Impedance matching a phased array-antenna over wide scan angles by connected circuits," *IEEE Trans. Antennas Propag.*, vol. AP-12, pp. 28–34, Jan. 1964.

[31] H. W. Bode, *Network Analysis and Feedback Amplifier Design*, Sec. 16.3, Van Nostrand, New York, 1945.

[32] R. M. Fano, "Theoretical limitations on the broadband matching of arbitrary impedance," *J. Franklin Institution*, vol. 249, pp. 57-83, Jan. 1950.

Nadia Haider received the B.Sc. (cum laude) in Electrical Engineering from Saxion Hogeschool Enschede, the Netherlands in 2007. She received the M.Sc. (cum laude) and Ph.D. degrees in Electrical Engineering from the Delft University of Technology, the Netherlands in 2010 and 2015, respectively.

Since 2009 Dr. Haider is with the Microwave Sensing, Systems and Signals group of Delft University of Technology. Her master graduation project focused on dual-polarized UWB antennas and her doctoral research focused on reconfigurable antennas. She has developed frequency reconfigurable L/S-band antennas with wide angle scanning capabilities for adaptive phased-array radars. Her main research interests have been antenna designs, active phased arrays, impedance matching and reconfigurable technologies.

Diego Caratelli was born in Latina, Italy on May 2, 1975. He received the Laurea (summa cum laude) and Ph.D. degrees in Electronic Engineering, as well the M.Sc. degree (summa cum laude) in Applied Mathematics from Sapienza University of Rome, Italy in 2000, 2004, and 2013, respectively. From 2005 to 2007, he was Research Fellow at the Department of Electronic Engineering, Sapienza University of Rome, Italy, where he was appointed as Contract Professor of Interdisciplinary Laboratory in 2007-2010. From 2007 to 2013, he was Senior Researcher at the International Research Centre for Telecommunications and Radar of Delft University of Technology, the Netherlands. In 2013 he co-founded The Antenna Company, where is currently Director of Research and Development. Since 2014 he is, also, Associate Professor at the Institute of Cybernetics of Tomsk Polytechnic University, Russia.

His main research interests include the full-wave analysis and design of passive devices and antennas for satellite, wireless and radar applications, the development of analytically-based numerical techniques devoted to the modelling of wave propagation and diffraction processes, as well as the theory of special functions for electromagnetics, the deterministic synthesis of uniform/aperiodic antenna arrays, and the solution of boundary-value problems for partial differential equations of mathematical physics. His research activity has so far resulted in more than one hundred publications in international journals, book chapters, and conference proceedings.

Dr. Caratelli was the recipient of the Young Antenna Engineer Prize at the 32th European Space Agency Antenna Workshop. He received the 2010 Best Paper Award from the Applied Computational Electromagnetics Society (ACES). He serves as reviewer for several international journals, and is a member of ACES, the Italian Electromagnetic Society (SIEm), and the Institute of Electrical and Electronics Engineers (IEEE).

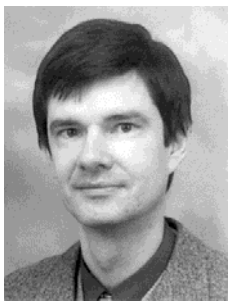

Alexander G. Yarovoy graduated from the Kharkov State University, Ukraine, in 1984 with the Diploma with honor in radiophysics and electronics. He received the Candidate Phys. & Math. Sci. and Doctor Phys. & Math. Sci. degrees in radiophysics in 1987 and 1994, respectively.

In 1987 he joined the Department of Radiophysics at the Kharkov State University as a Researcher and became a Professor there in 1997. From September 1994 through 1996 he was with Technical University of Ilmenau, Germany as a Visiting Researcher. Since 1999 he is with the Delft University of Technology, the Netherlands. Since 2009 he leads there a chair of Microwave Sensing, Systems and

Signals. His main research interests are in ultra-wideband microwave technology and its applications (in particular, radars) and applied electromagnetics (in particular, UWB antennas). He has authored and co-authored more than 250 scientific or technical papers, four patents and fourteen book chapters. He served as a Guest Editor of five special issues of the IEEE Transactions and other journals. Since 2011 he is an Associated Editor of the International Journal of Microwave and Wireless Technologies.

Prof. Yarovoy is the recipient of the European Microwave Week Radar Award for the paper that best advances the state-of-the-art in radar technology in 2001 (together with L.P. Ligthart and P. van Genderen) and in 2012 (together with T. Savelyev). In 2010 together with D. Caratelli Prof. Yarovoy got the best paper award of the Applied Computational Electromagnetic Society (ACES).

Prof. Yarovoy served as the Chair and TPC chair of the 5th European Radar Conference (EuRAD'08), Amsterdam, the Netherlands, as well as the Secretary of the 1st European Radar Conference (EuRAD'04), Amsterdam, the Netherlands. Prof. Yarovoy served also as the co-chair and TPC chair of the Xth International Conference on GPR (GPR2004) in Delft, the Netherlands. Since 2008 he serves as Director of the European Microwave Association (EuMA).